



HAL
open science

Impact of NaCl spray on the durability of PEMFC single cells and stacks in marine environment

Marie Lamard, Bruno Auvity, Paul Buttin, Sébastien Rosini, Clement Retiere

► To cite this version:

Marie Lamard, Bruno Auvity, Paul Buttin, Sébastien Rosini, Clement Retiere. Impact of NaCl spray on the durability of PEMFC single cells and stacks in marine environment. *Journal of The Electrochemical Society*, 2023, 170, pp.024504. 10.1149/1945-7111/acb8e0 . cea-04001007

HAL Id: cea-04001007

<https://cea.hal.science/cea-04001007>

Submitted on 22 Feb 2023

HAL is a multi-disciplinary open access archive for the deposit and dissemination of scientific research documents, whether they are published or not. The documents may come from teaching and research institutions in France or abroad, or from public or private research centers.

L'archive ouverte pluridisciplinaire **HAL**, est destinée au dépôt et à la diffusion de documents scientifiques de niveau recherche, publiés ou non, émanant des établissements d'enseignement et de recherche français ou étrangers, des laboratoires publics ou privés.

Title: Impact of NaCl Spray on the Durability of PEMFC Single Cells and Stacks in Marine Environment

Marie Lamard^{1, 2, z}, Bruno Auvity², Paul Buttin¹, Sébastien Rosini³, and Clément Retière¹

¹ CEA, département Pays de la Loire, F-44340 Bouguenais, France

² Nantes Université, LTeN (CNRS UMR 6607), Polytech Nantes, F-44300 Nantes, France

³ Univ Grenoble Alpes, CEA, LITEN, F-38000 Grenoble, France

^z Email: Marie.LAMARD@cea.fr

Abstract Text

The present work investigates the effects of a salt spray injected into the airflow of Proton Exchange Membrane Fuel Cells (PEMFCs) at various time scales and contamination levels, with the long-term objective of identifying the appropriate protection of fuel cells for maritime applications. A dedicated experimental setup generates a sodium chloride (NaCl) mist in the cathode airflow to contaminate single cells and stacks. Constant current density tests led to lifetime shortening with partial recovery after cathode rinsing. Then, Membrane Electrode Assemblies (MEAs) post-mortem characterizations revealed that NaCl was present in the cathode gas diffusion layer, and chlorine reached the catalyst layer for high concentrations. Furthermore, chlorides enhanced current collectors and bipolar plates (BPs) degradation, as corrosion products were identified in MEAs and stack effluents. A sailboat propulsion stack operated 50 hours at sea was meanwhile analyzed. As for the laboratory work, chlorine and stainless steel from BPs were found in MEAs, comforting the idea that the marine environment can damage fuel cells. Overall, this study evidences that NaCl effects on PEMFCs not only depend on the concentration but also on the MEA type, plate material, and startup/shutdown procedure.

Introduction

In the context of global warming, there is an urgent need to find solutions to reduce air contamination. Indeed, the Intergovernmental Panel on Climate Change (IPCC) reported that carbon neutrality must be achieved around 2050 to limit global heating to 1.5°C by 2100.¹ For this purpose, improving the durability of technologies as Proton Exchange Membrane Fuel Cells (PEMFCs) is essential. They produce electricity thanks to dioxygen (O₂) and dihydrogen (H₂) by only rejecting pure water and heat. In this sense, water electrolysis is ideal for H₂ production, when carried out with green electricity.^{2,3} However considered the most mature fuel cell (FC) type, there are still some issues concerning PEMFC. Work has been done on the catalyst to address cost issues,⁴ including platinum (Pt) recycling⁵ and the use of sustainable compounds.⁶ Concerning durability, the study of specific environmental effects is consistent with the wide range of industrial applications. More precisely, FCs are mostly fed with O₂ from the air, which may contain particles or gases that can reduce their performance.

The focus of this study is the impact of an aggressive environment, the marine atmosphere, on PEMFC single cells and stacks. Indeed, even if companies are interested in this technology for maritime transportation, various air pollutants are found in harbors, such as sulfur dioxide and nitrogen oxides,⁷ which were proven to affect PEMFC performance.^{8,9} The proximity of

the sea also implies the presence of specific potential contaminants, such as sea salt. When the PEMFC cathode is fed with marine air, atmospheric aerosols containing sodium chloride (NaCl)¹⁰ reach the membrane electrode assembly (MEA). However, few studies have addressed the problem of NaCl contamination. As reported by Mikkola et al.,¹¹ chlorides (Cl⁻) did not affect as much as expected the MEA of a single cell. In spite of that, an increase in the high-frequency resistance was detected and explained by the presence of sodium ions (Na⁺) in the membrane. Nine years later, Sasank et al.¹² revealed that seawater droplets reduced by 60% the performance of an open-cathode PEMFC stack, after 48 hours of contamination. Then, a clean water rinsing helped to recover 87% of the initial performance. In line with these results, Uemura et al.¹³ observed a degradation after NaCl particle injection at the cathode side of a single cell. The cathode active area (ECSA) was decreased by 22.6% after fifty minutes of contamination. Yan et al.¹⁴ also highlighted NaCl effects, but the authors pointed out that the CaCl₂ impact was more considerable. Even if care should be taken when comparing these investigations realized under different experimental conditions, NaCl injection seems to reduce PEMFCs performance.

Some contamination tests were carried out with hydrochloric acid (HCl), which provided further information on Cl⁻ interaction with PEMFCs. Based on Matsuoka et al. work,¹⁵ chlorides significantly affected single cell performance, contrary to fluoride, sulfate, and nitrate contaminations. Decreases in cell voltage and ECSA were noticed, as well as Pt dissolution at the air inlet side. Li et al. confirmed these observations, with an increase in Pt particle size after HCl contamination.¹⁶ Further investigations on operating conditions demonstrated that higher current densities and HCl concentrations, and lower moisture contents resulted in a loss of performance.¹⁷ Concerning performance recovery, Steinbach et al.¹⁸ established that regeneration depends on the catalyst type, supporting the idea that complex interactions exist between Cl⁻ and the catalyst layers (CLs). On another note, NaCl is frequently used to accelerate the degradation of SS316L in experimental work.¹⁹ Stainless steel bipolar plates (BPs) corrosion triggers iron release, which can participate in a Fenton reaction and provoke membrane degradation.²⁰

Overall, Na⁺ can dehydrate the membrane by blocking sulfonate sites^{11,21} whereas Cl⁻ affects the catalyst by adsorption or dissolution-redeposition of Pt particles, leading to ECSA loss.^{13,15–18,22} However, the degradation mechanisms require clarification, and the NaCl amount reaching the FC was very high compared to marine environments,¹¹ or not even specified¹². Moreover, the work referenced above mostly focused on CLs contamination. To our knowledge, there is no complete study of the impact of a NaCl spray on PEMFCs at single cell and stack scales, with a final comparison with a FC operated in a marine environment.

Therefore, the objective of this experimental work is to verify and explain the trend of performance degradation for both single cells and stacks, when exposed to a NaCl mist. The final aim is to predict the adaptations needed for PEMFC deployment in marine environments. Although specific FC air filters are commercialized, no clear exposure limit is precisely defined. In these conditions, close attention was paid to the NaCl quantity injected into the airflow thanks to a dedicated experimental setup carefully qualified. Then, single cells and stacks contamination tests were carried out for various NaCl concentrations in the air (0.01 to 5 g/m³) and duration times (0.5 to 160h), at constant current density. In our approach, two types of MEAs and two current collectors (CCs) pairs were used and compared for single cells. Indeed,

a graphite CC was put at the cathode side to discriminate NaCl effects from corrosion products ones, which were released by gold-plated copper CCs. Finally, electrochemical tests and post-mortem analyses helped to evaluate the mechanisms that might be implied in the degradation. MEAs from a ship propulsion stack exposed to a real marine environment were additionally observed, which deterioration reinforced the pertinence of this study.

Experimental

Contamination Setup.—A dedicated setup was conceived and realized for polluting PEMFC single cells and stacks, in order to study the impact of a NaCl mist injected into the feeding airflow. To this end, some authors used a pump to spray the contaminant. Mikkola et al.¹¹ published one of the first studies of NaCl effects on an operating PEMFC, which setup included a pump delivering a constant flow of NaCl solution. Similarly, Li et al.^{16,17} injected HCl solutions with a pump to contaminate both the cathode and anode. This method was investigated for single cells, but the airflow was not high enough to create a mist, which posed a risk of cell flooding. One way to avoid flooding was provided by a few experimental studies,^{13,14} with the use of an ultrasonic vibrator that usually sprays droplets in the micrometer range.²³

Consequently, an ultrasonic vibrator was selected to generate the NaCl mist. Although in many ways similar to Uemura et al. setup,¹³ adjustments were made to inject a mist instead of solid particles, but also to be easily connected to the test benches when needed. Moreover, most of the couplings and tubes were chosen with chemically stable materials, to prevent the injection of corroded metallic impurities. **The experimental setup integrated in the single cell test bench is represented in Figure 1.** The ultrasonic vibrator creates a NaCl mist in a buffer tank flushed by the airflow, which carries the salt spray. **It was not put into the tank to prevent metal parts from corrosion and induced FC contamination by corrosion products.** The droplets diameter was about 5 μm , as specified by the manufacturer. NaCl solutions to be sprayed were prepared with deionized water at several concentrations. They were linked to the final content of NaCl in the airflow thanks to qualification tests carried out. On another note, the FC air input did not include any filter, as the objective was to observe the impact and the potential damages caused by a NaCl mist.

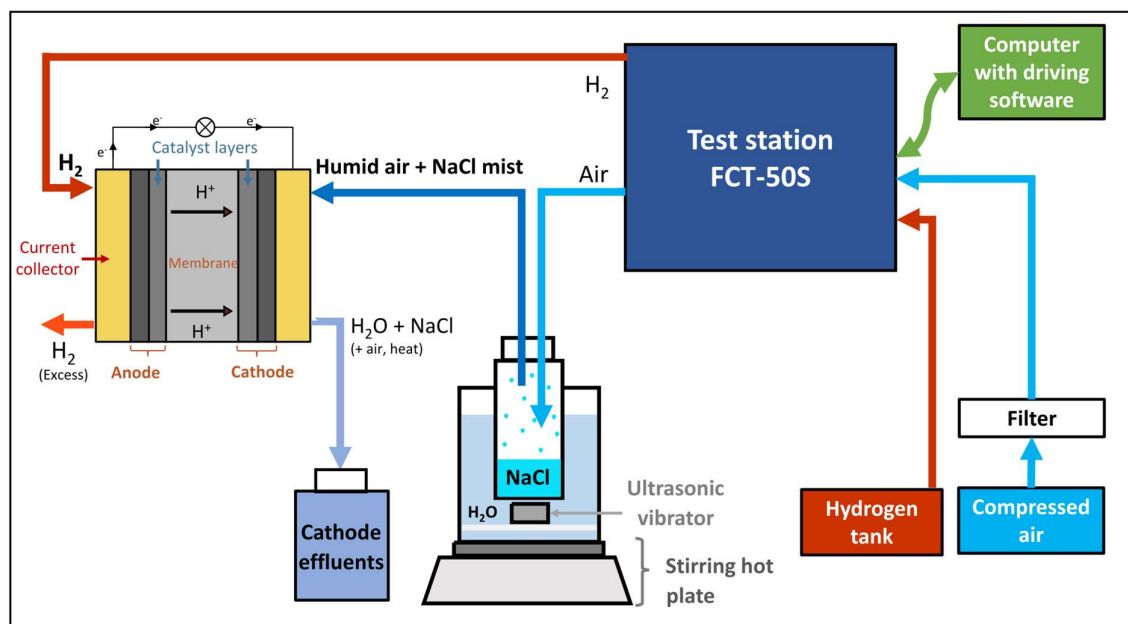


Figure 1. Experimental setup used for PEMFC contamination integrated in the single cell test bench.

Experimental Setup and Fuel Cells Specifications.—Single cells selected for the tests have an active area of 11.76 cm² (19.6 x 0.6 cm) and were mounted on the setup presented in Chevalier et al. work,²⁴ without the segmented channels. Two types of MEA were studied, from different suppliers, to compare their durability when exposed to NaCl. Type 1 has a Pt loading of 0.5 mg/cm² for both electrodes, whereas type 2 Pt amount is 0.4 mg/cm² for the cathode and 0.1 mg/cm² for the anode. It should be noted that MEAs type 1 were stored for four years without specific precautions, which could have caused some damage and limited reproducibility of performance. Oppositely, MEAs type 2 were fresh and specially ordered for this study. Copper CCs coated with a gold thin film were initially used, with two straight channels for the gases. As noted by Georges et al.,²⁵ the gold coating may contain defects that make the underlying layers vulnerable. Therefore, a graphite plate, more adapted to severe environments, subsequently replaced the copper CC at the cathode. The anode one was kept, as it was not directly exposed to the NaCl spray. All of the experiments were performed with a Biologic/Paxitech instrument (FCT-50S) driving the FC. To preserve the equipment from corrosion during contamination tests, the air outlet containing NaCl traces was not connected back to the test station. It offered a means of collecting cell effluents, even though it did not allow tests under pressure.

NaCl mist contamination tests were also carried out on PEMFC stacks to investigate the distribution of impacts. Stacks were constituted of five cells with MEA type 2 of 220 cm² (hereinafter C1, C2, C3, C4, and C5). The geometry was different from the single cell setup, but the MEA composition was the same. BPs were made of 316L stainless steel partially covered with graphite to improve the conductivity. All MEA, CC, and BP configurations tested are summarized in Table I. Stack scale experiments were conducted with a homemade test bench from CEA LITEN, commonly used for single cells and low-power stacks. Stack inlets

and outlets were localized on the anode endplate side, closest to the C1. As for the single cells, effluents were collected at the air outlet to prevent the test bench from deteriorating.

Table I. Summary of the specifications of the fuel cells used for both scale studies.

Type of membrane electrode assembly	Platinum amount (mg/cm ²)	Scale studied	Current collectors or bipolar plates tested	Remarks
Type 1	0.5 (cathode and anode)	Single cells	Copper	Stored for four years without specific measures
Type 2	0.4 (cathode) 0.1 (anode)	Single cells and stacks	Copper, graphite Stainless steel 316L	Specially ordered for the project

Testing procedures.—Constant current density tests were made at 0.5 A/cm² when polluting the airflow. After a conditioning step provided by the supplier, the FC was operated for approximately 20h at 0.5 A/cm² to ensure that MEA conditioning was sufficient for obtaining a stable performance. The operating conditions were at temperature of 60°C (for both gas lines and cell), relative humidity (RH) of 75% (single cells) and 50% (stacks), stoichiometry H₂/O₂ of 1.5/5 (single cells) and 1.5/2 (stacks), and minimum flow rates of 100 and 500 mL/min respectively for single cells.

The contamination setup was filled with deionized water and connected to the cathode for acquiring a baseline. Then, pure water was replaced by a NaCl solution (0.1 to 50 g/L) for accelerated degradation tests. This corresponds to a NaCl amount from 10 to 5 000 mg/m³ in the airflow, as determined thanks to qualification experiments performed on the contamination setup. Degradation tests were carried out at 0.5 A/cm², with no additional cathode humidification.

To highlight the NaCl impact, several electrochemical tests were combined during various contamination stages. Polarization curves were plotted to track the overall variation in performance. They were recorded in a galvanostatic mode for stacks. Oppositely, single cell polarization curves were obtained in potentiostatic mode, with increments of 0.04 V every 60 s. This method ensures interpretable results, even for severely degraded cells that cannot provide high currents.

To complement the information given by polarization curves, electrochemical impedance spectroscopy (EIS) spectra were recorded. Indeed, Li et al. EIS study¹⁷ showed that chloride contamination affects the charge and mass transfer resistances, but not the PEMFC membrane conductivity. EIS spectra were obtained for all cells at 0.05 A/cm² and 0.4 A/cm², to study both kinetics and mass transport phenomena. The frequency range was 2000 to 0.350 Hz with a signal amplitude equal to 10 % of the stationary current set point. Randles equivalent circuit was used to fit the data collected.

In order to determine the available surface area of the catalyst, cyclic voltammetry (CV) was completed at the cathode for the stacks study only, because of the setup configuration. The voltage sweep range was 0.06 to 0.7 V at scan rates of 50, 100, and 200 mV/s. Three scans were recorded for each cell and each testing condition. CV was also carried out at 1 mV/s, to study the evolution of H₂ crossover and thus the membrane state of health. Operating conditions for CV recordings were 50% RH with H₂ and N₂ flow rates of 0.070 m³/h and 0.23 m³/h

respectively.

The FCT-50S was directly driving the characterization procedures and recordings for single cells. These cells were humidified with clean water to avoid degradation during the tests. It was recognized that inevitable condensation droplets can momentarily clog the tube at the cathode entrance because of the low flow rate, resulting in a slightly noisy signal for EIS at 0.05 A/cm². Fortunately, this phenomenon is acceptable when studying the NaCl contamination itself or the FC global performance. On another note, procedures were controlled via an Autolab potentiostat to achieve EIS and CV recordings for each cell of the polluted stacks. As flow rates were higher than for single cells, clogging did not occur at this scale.

Scanning Electron Microscopy (SEM) analyses coupled with Energy Dispersive X-Ray Spectroscopy (EDS) were carried out on MEAs and effluents. These observations were supplemented by conductivity measurements, as in Pozio et al. work.²⁰ Cathode effluents were put into a drying oven to obtain a powder. Although NaCl cannot be quantified using these post-mortem analyses because of the presence of other chemical components, they enabled its identification in contaminated FCs. MEAs samples were coated and polished, thus obtaining a precise cross-sectional view to look for potential delaminations. Then, samples were peeled to observe rigorously each layer. For single cells, both extremities were observed, whereas entrance, middle, and air outlet were studied for stacks.

Results

Single cells and PEMFC stack contaminations were realized thanks to the dedicated setup mentioned earlier. Besides, a solution for discriminating the direct and indirect effects of NaCl on PEMFCs will be explored in this paper.

Single cells.—As described above, two types of MEAs were studied for various time scales and contamination rates thanks to the specific setup injecting NaCl mist in the cathode airflow.

30 minutes exploratory tests were carried out on MEA type 1 mounted with gold/copper CCs, with an approximate NaCl amount in the airflow of 10 and 5 000 mg/m³. When the cell performance loss was about 0.1 V from the baseline, the contamination test was stopped and the cathode was humidified with deionized water again. As shown in Figure 2 (a), 10 mg/m³ NaCl during 30 minutes did not trigger perceptible loss of performance. It should be noted that the baseline signal fluctuates. As explained before, this is due to a condensation issue in the tubes and does not affect the global performance. The performance obtained during the baseline recording was about 0.38 V, which was not as high as expected for PEMFCs operated at 0.5 A/cm². The only explanation that can be given was the use of an old MEA, as described earlier.

Conversely, 5 000 mg/m³ NaCl provoked a sudden and severe drop in voltage from 0.36 to 0.1 V. Then, signal stabilization was observed a few minutes after the end of nebulization. Finally, deionized water humidification allowed a voltage recovery of 84%. Unexpectedly, the single cell recovered fully its initial performance, reaching 0.45 V at 0.5 A/cm², after a week of washing procedures (conditioning cycles with changes in gas flow rate, pressure, and RH).

This value is higher than the baseline one, presumably because the conditioning time was too short.

Similar experiments were run with a MEA type 2 (Figure 2 (b)). This time the baseline voltage reached 0.65 V for a current density of 0.5 A/cm², as expected for PEMFCs. As for type 1, a 10 mg/m³ contamination did not trigger any decrease in voltage in 30 min. Then, the 5000 mg/m³ NaCl impact was not sudden and the exposure lasted 30 min in order to lose 0.1 V. Surprisingly, the voltage drop continued during the entire regeneration attempt under pure water. Even if identical setup and operating conditions were used for type 1, this effect did not appear. This could be explained by NaCl remaining in the tubes or in the cathode GDL, as the contamination was four times longer for type 2. Partial recovery of performance was nevertheless obtained after rinsing procedures, with a signal fluctuating around 0.29 V. Although the recovery got off to a good start, complete regeneration was not completed for type 2 after more than 30h of rinsing procedures.

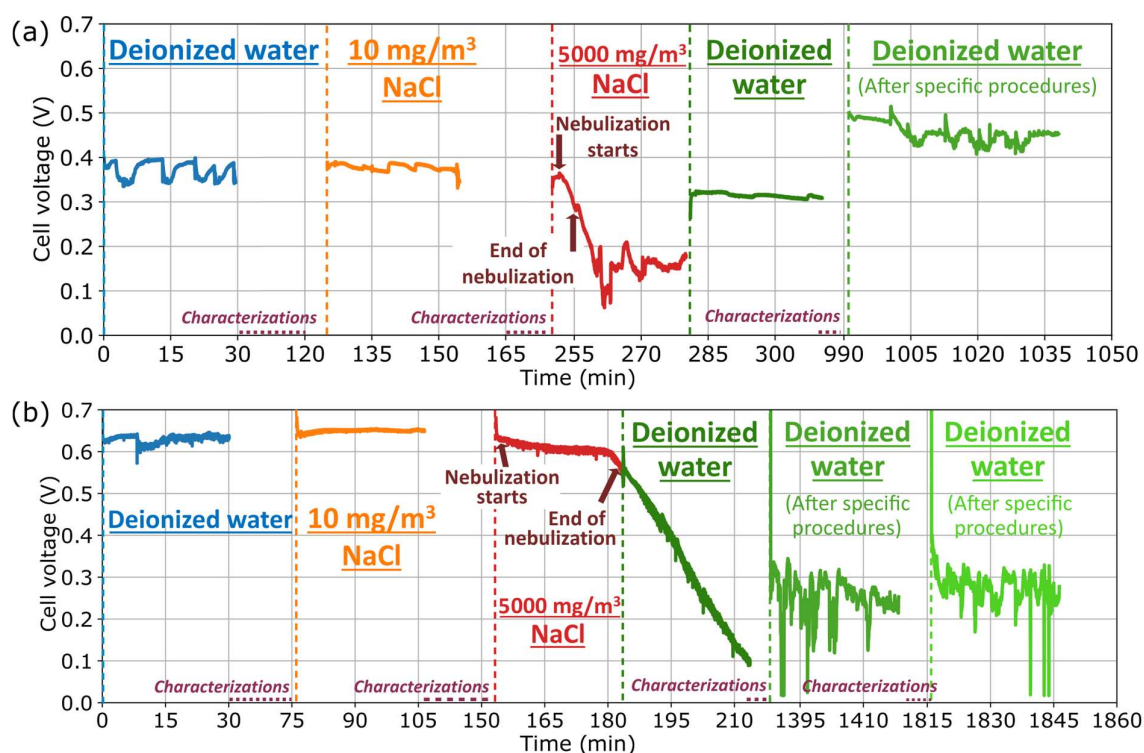


Figure 2. Single cell voltage time evolution depending on NaCl concentration for (a) membrane electrode assembly type 1 and (b) type 2. Operating conditions: 0.5 A/cm², 60°C, relative humidity of 75%, stoichiometry 1.5/5 H₂/O₂ with minimum flow rates of 100 and 500 mL/min.

After the exploratory study, longer contamination tests were undertaken at 10 mg/m³ NaCl air content on both MEA types with copper CCs, as illustrated in Figure 3. This concentration is approximately 200 times higher than in a natural marine environment. MEA type 1 was polluted for 24h, with night breaks. The voltage decrease was about 24 mV/h during the contamination step. In addition, nitrogen (N₂) flush induced a 68 % recovery of the initial

voltage. Unpredictable increases or decreases in performance were observed when restarting the FC, which will be explored in further investigations.

Concerning MEA type 2, shutdowns were done only every weekend after the first 90h of contamination. As for type 1, partial recovery was visible after restarts, except for the first weekend (29h) where membrane dehydration occurred, presumably not linked to the NaCl presence. After 165h of contamination with an average voltage decrease of 3.3 mV/h, the FC was operated with deionized water for 30h. The voltage drop has been halved (1.7 mV/h) but remained non-negligible. Contrary to highly concentrated and short duration experiments, this recovery method is unlikely to be efficient. However, as for the type 1 MEA, 30min of N₂ rinsing helped to recover about 80% of initial performance.

Characterization tests were carried out on both MEAs although they did not yield additional information. Even if it was difficult to compare the results as the initial performance and contamination time were different, the degradation rate of MEA type 1 was about 8 times higher. This result supports the idea that type 2 was likely to be more robust.

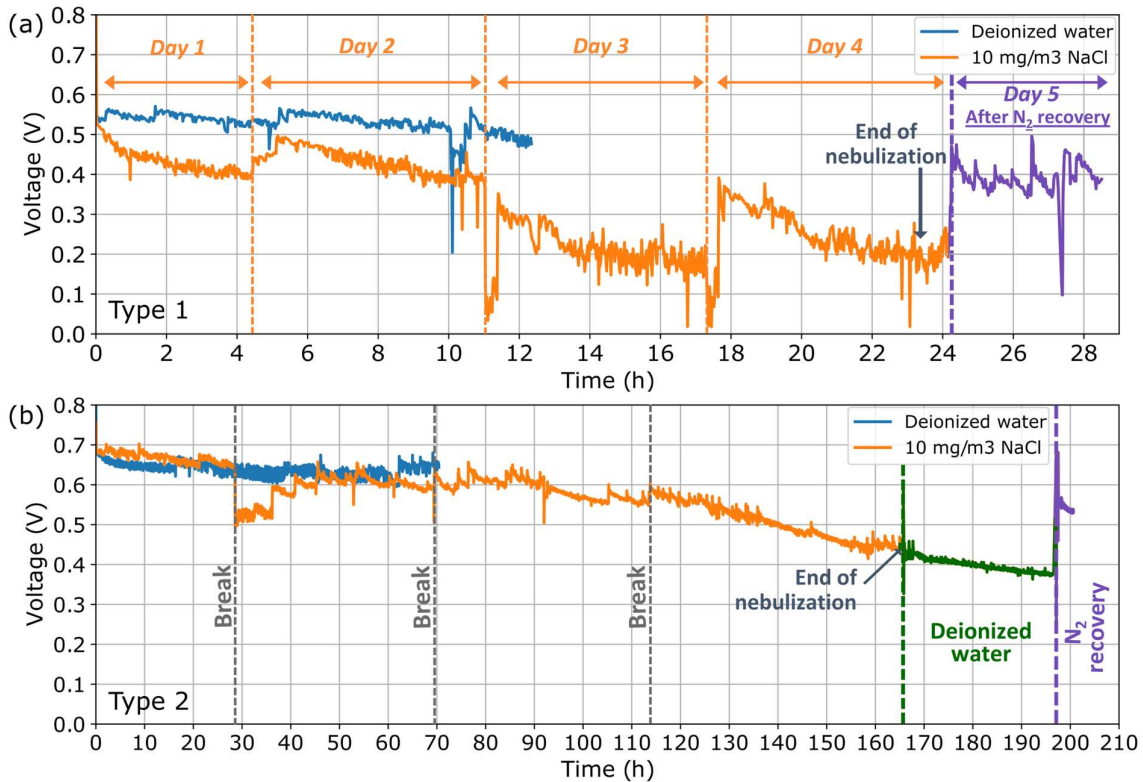


Figure 3. (a) Single cell voltage time evolution with a 10 mg/m³ NaCl contamination for membrane electrode assembly type 1 and (b) for type 2. Operating conditions: 0.5 A/cm², 60°C, relative humidity of 75%, stoichiometry 1.5/5 H₂/O₂ with minimum flow rates of 100 and 500 mL/min.

Both experiments highlighted a decrease in PEMFC performance with partial recovery after a clean mist rinsing. However, as outlined before, the use of gold-plated CCs can affect the FC by releasing corrosion products during NaCl contamination tests. Therefore, a slightly different

single cell setup was realized to discriminate the NaCl direct impact on the MEA and the indirect corrosion particle effects. As explained in the previous section, a graphite plate was mounted at the cathode with a type 2 MEA.

Contamination tests were carried out in this configuration with 10 mg/m^3 NaCl. The evolution of the cell voltage as a function of time is shown in Figure 4 (a) for the entire contamination test. In accordance with the previous results, there was a significant decrease in performance when the single cell was exposed to the NaCl mist, with a degradation rate of 2.2 mV/h . The polarization curves recorded at various contamination times (Figure 4 (b)) confirmed that no more than 50h of continuous pollution provoked a drastic performance loss. Surprisingly, the open circuit voltage dropped to 0.76 V when restarting the single cell after 122h of contamination and a weekend break. As shown by the corresponding polarization curve, it appears that the kinetic and ohmic contributions were strongly limiting. Pure water humidification did not lead to performance recovery this time. These results nevertheless corroborate the direct impact of NaCl on PEMFCs.

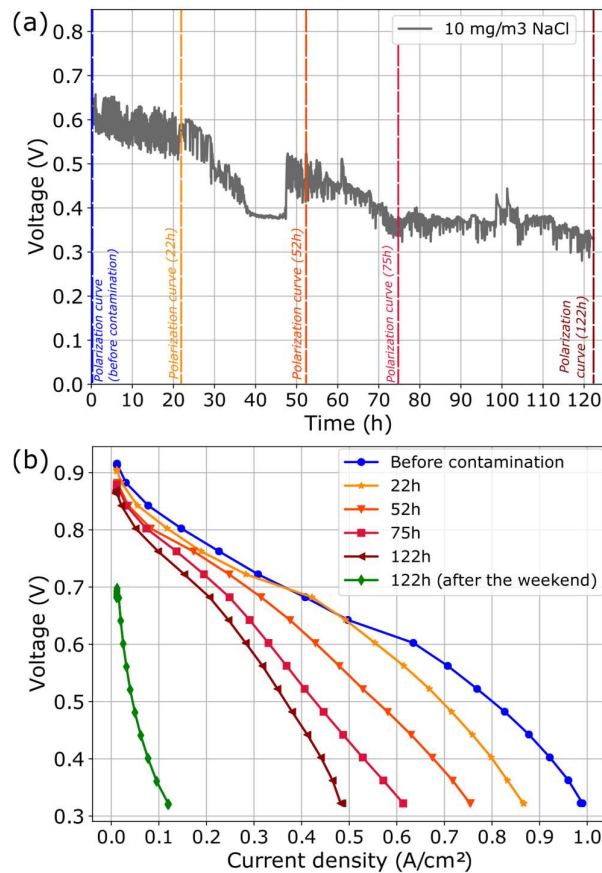


Figure 4. (a) Contamination time dependence on the voltage at 0.5 A/cm^2 and (b) polarization curves associated for a single cell assembled with a graphite current collector at the cathode. Operating conditions: MEA type 2, 10 mg/m^3 NaCl, 60°C , relative humidity of 75%, stoichiometry $1.5/5 \text{ H}_2/\text{O}_2$.

Stacks.—To study NaCl impact on more powerful systems, comparable experiments were carried out on stacks. A reference stack was operated for 360 h under pure water humidification at 0.5 A/cm², showing stable performance with a negligible voltage drop of 0.012 mV/h. To study the overall effect of high contaminant levels, a stack with fresh MEAs was exposed to a 5000 mg/m³ NaCl mist. Contrary to the baseline stack behavior, inspection of Figure 5 (a) indicates that cell voltages oscillated after no later than 3 h of contamination meanwhile outgoing effluents started getting orange. The stack became unusable after 8 h, because of C4 sudden voltage drop, after recording a polarization curve.

Surprisingly, a characterization cycle composed of CV, EIS, and polarization curves measurements under pure water humidification helped to recover 95% of the overall stack performance. The regeneration was not complete for C3 and C4, which were the most degraded cells.

Another fresh stack was polluted with 500 mg/m³ NaCl, to explore a longer recovery procedure. As pointed out in Figure 5 (b), a first 30h contamination step resulted in unstable voltage after 10h, followed by a sharp voltage drop for C5. As for the previous experiments, this degradation was accelerated during a polarization curve recording. Then, an excellent performance recovery of 96% was obtained after characterization cycles and 13 h of operation under pure water mist humidification. When the effluents became again colorless, a second contamination was investigated. In this case, the C5 signal was unstable as soon as the contamination started. The test lasted only 13 h, with an overall voltage drop due to C1 and C5 failures. Once more, an overwhelming regeneration of 95% was observed.

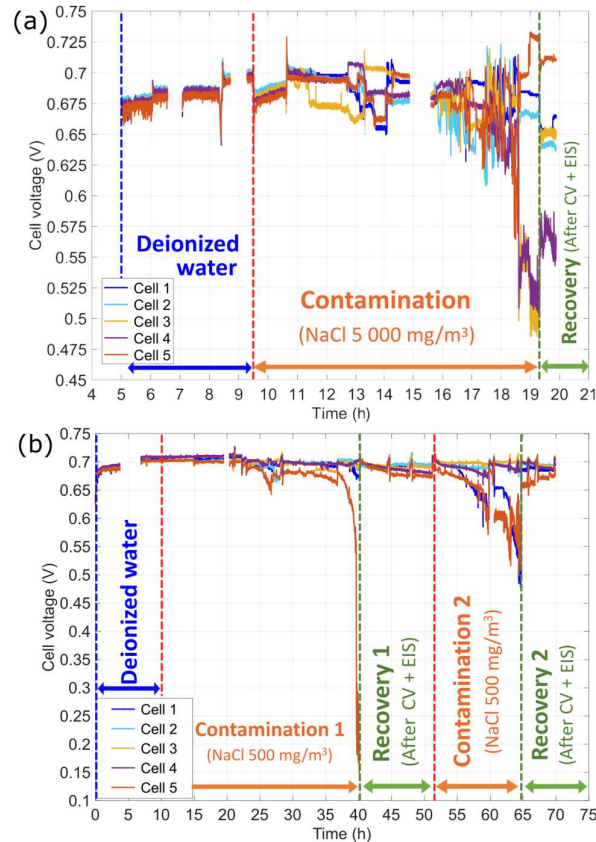


Figure 5. (a) Cell voltage time dependences for a 5000 mg/m³ and (b) for a 500 mg/m³ NaCl contamination (0.5 A/cm², 60°C, relative humidity of 50%, stoichiometry 1.5/2 H₂/O₂).

The most relevant polarization curves recorded before and after each contamination and recovery step can be found in Figure 6 (a). The plots of the polarization curves saved after recovery 1 and recovery 2 are overlapped. This graph highlights the excellent recovery obtained after both contamination steps, although a small activation loss remained. As evident when comparing Nyquist plots represented in Figure 6 (b) and (c), the C5 mass transfer semi-circle was extremely large after the first contamination. The mass transfer resistance was multiplied by 20 but was fully recovered after rinsing. Conversely, it seems that C4 performance has continued to decline during the recovery step. No significant change was noticed in high frequency resistance (HFR), except for C1, whose HFR increased by 1.3.

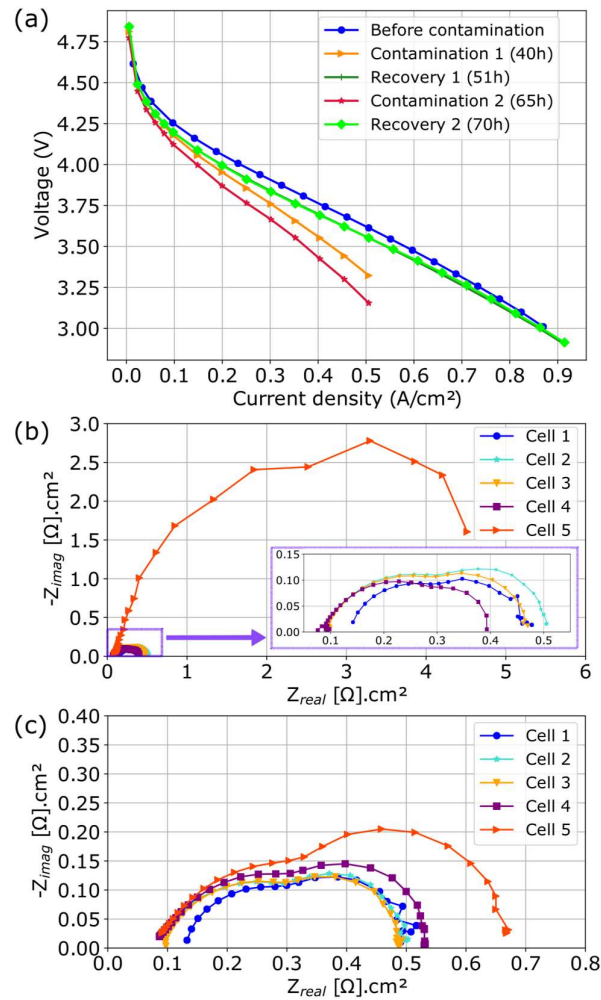


Figure 6. (a) Polarization curves of the stack contaminated by 500 mg/m³ NaCl. (b) Electrochemical impedance spectroscopy spectra recorded at 0.4 A/cm², at the beginning of recovery 1 (40h) and (c) at the end of recovery 1 (51h). Operating conditions: 60°C, relative humidity of 50%, stoichiometry 1.5/2 H₂/O₂.

Permeation tests were carried out on both stacks for various contamination times. For the most degraded cells, the permeation current rose from approximately 40 to 50 mA between initial and final measurements. Concerning the cathode CV tests, the ECSA values were not reduced with NaCl contamination (Figure 7). Surprisingly, for the most degraded cells of the 500 mg/m³ study (C1 and C5), the ECSA slightly increased after NaCl exposure and decreased under clean mist operation for both phases. For example, it increased from 56.8 m²/g to 64.9 m²/g after the first contamination for C5, and decreased to 57.4 m²/g after rinsing. The first scans were also exploited to eliminate the possibility of other electrochemical processes happening during the first voltage sweep, but a comparable behavior was obtained. This controversial result was not caused by insufficient conditioning time to activate the reaction sites. Indeed, the ECSA calculated for the reference stack remained between 54 and 58 m²/g after 360 h of operation with deionized water mist (not represented).

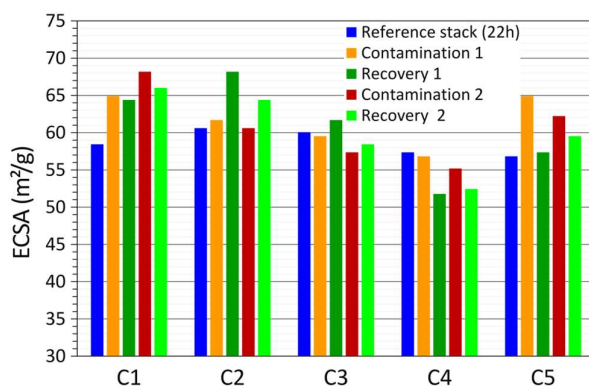


Figure 7. ECSA obtained with cathode cyclic voltammetry measurements at various stages of 500 mg/m³ NaCl contamination (third scan, 50 mV/s, 60°C, relative humidity of 50%, H₂ and N₂ flow rates of 0.070 m³/h and 0.23 m³/h respectively).

Post-mortem analyses.—The single cell contaminated during the exploratory study was characterized by SEM-EDS. As illustrated in Figure 8 (a), MEA sectional view shows a delamination between the gas diffusion layer (GDL) and the cathode catalyst layer (CCL). NaCl was identified on the GDL and chlorine significantly reached the CCL. Various metallic species including gold were detected on the GDL surface, as well as deposits containing Ni, Fe, Cr, and Cd (Figure 8 (b)). Furthermore, copper was strikingly found in the CCL. Concerning the three MEAs contaminated with 10 mg/m³ NaCl, chlorine was detected on the surface of the cathode GDL. Ni, Au, and Cu were also identified when using a gold-plated CC. As expected, metal impurities were not present with a graphite one.

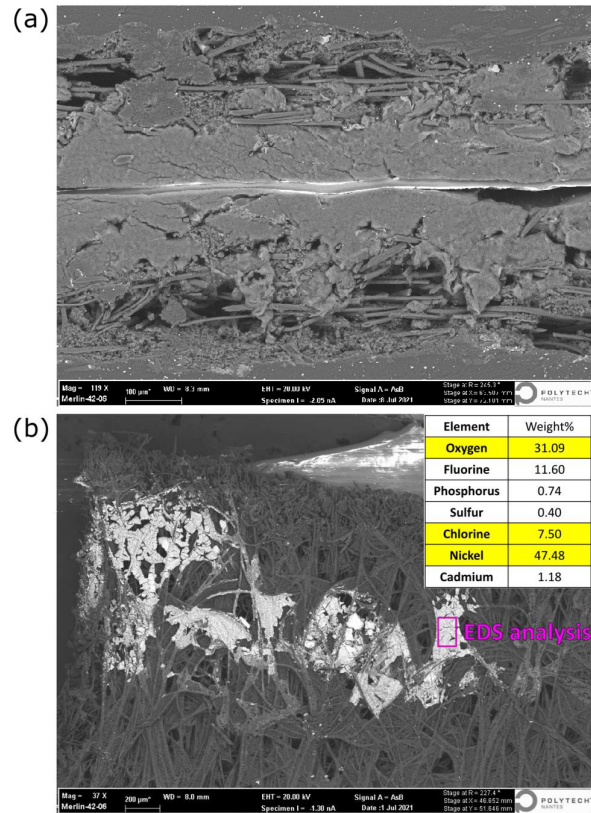


Figure 8. (a) Scanning electron microscopy images of the membrane electrode assembly (type 1) contaminated with NaCl during the exploratory study, from a cross-sectional view and (b) a view of the cathode gas diffusion layer surface, with Energy Dispersive X-Ray Spectroscopy analysis.

Observations were also undergone on collected effluents and C4, which was the most degraded of the 5000 mg/m³ NaCl polluted stack. A preliminary observation with the naked eye revealed an orange coloration of the collected effluents. Then, a mixture of white and orange powders was obtained after effluent drying. NaCl and corroded stainless steel (Fe, Cr, and Ni) were respectively detected, thanks to SEM coupled with EDS. As illustrated in Figure 9 (a), the BPs were corroded, especially close to the air inlet. The analyses confirmed the predicted link between the effluents impurities and these corrosion marks, which were identified as NaCl and stainless steel corrosion products (O, Fe, Cr, Ni, and Mo).

As evident from the MEA cross-sectional view in Figure 9 (b), GDL and CCL were strongly delaminated. This degradation was also visible to the naked eye on each MEA of the stack. Moreover, particles composed of Na, Cl, Fe, and Cr were found on the cathode GDL and micro-porous layer surfaces at the air inlet (Figure 9 (c)). As for single cells, chlorides reached the CCL. However, impurities were only present on the cathode GDL surface in the middle of the cell, and neither element was encountered at the air outlet. Likewise, all the MEA portions studied were clean on the anode side.

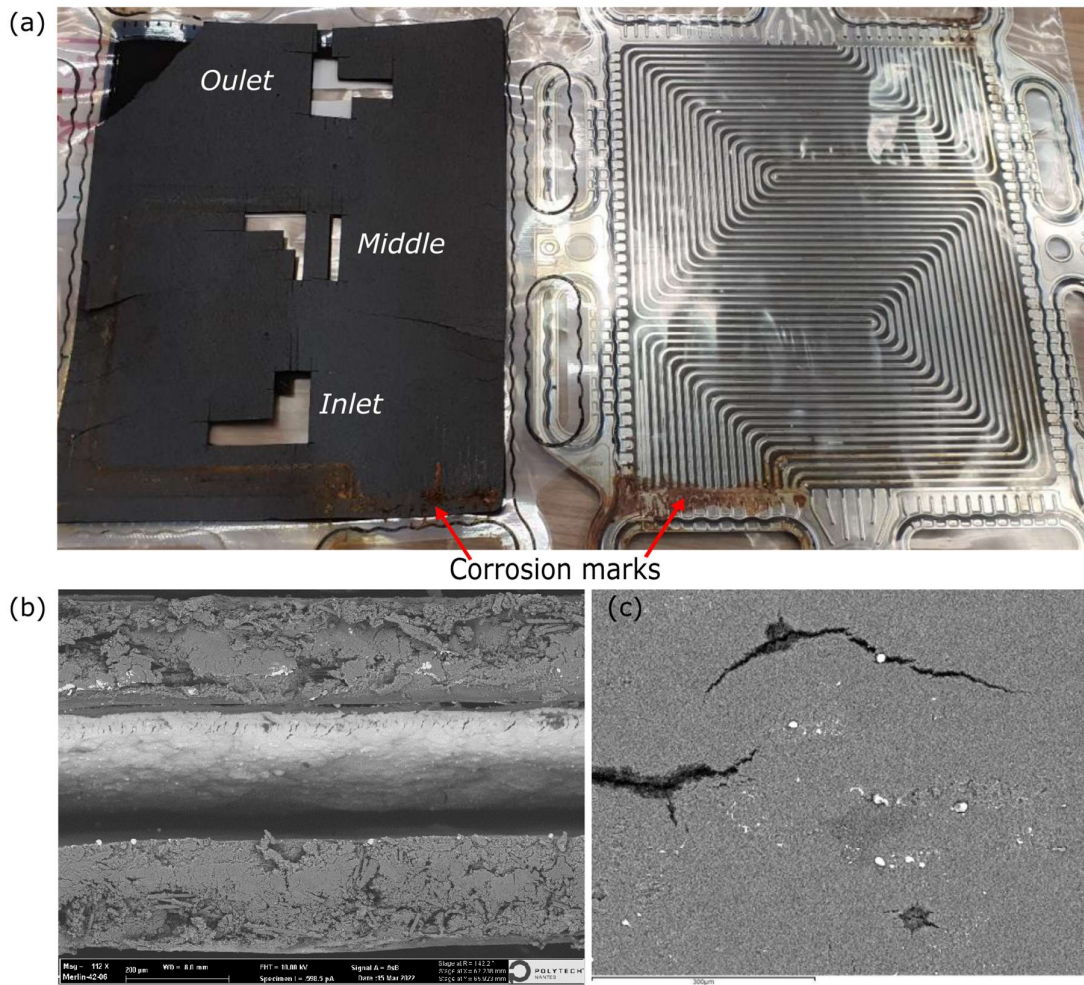


Figure 9. (a) Picture of the cathode membrane electrode assembly and bipolar plate contaminated with 5000 mg/m^3 NaCl. (b) Scanning electron microscopy observations of a cross-section and (c) cathode micro-porous layer close to the air inlet.

Beyond the scope of this study, a 35 kW PEMFC stack used for ship propulsion 10 years ago was analyzed. MEAs were vacuum-packed in 2015 to avoid unintended degradations. Even if performance did not decrease after 50h of operation in a marine environment, post-mortem characterizations revealed surprising observations. Indeed, as for laboratory tests, corrosion marks from BPs were visible on the MEAs (Figure 10) and identified as Fe, Cr, Ni, and Mo again combined with Cl, in the cathode GDL and microporous layer (MPL). In that respect, BPs were irreversibly damaged. This result provides the first evidence of PEMFC degradation when deployed for a maritime application.

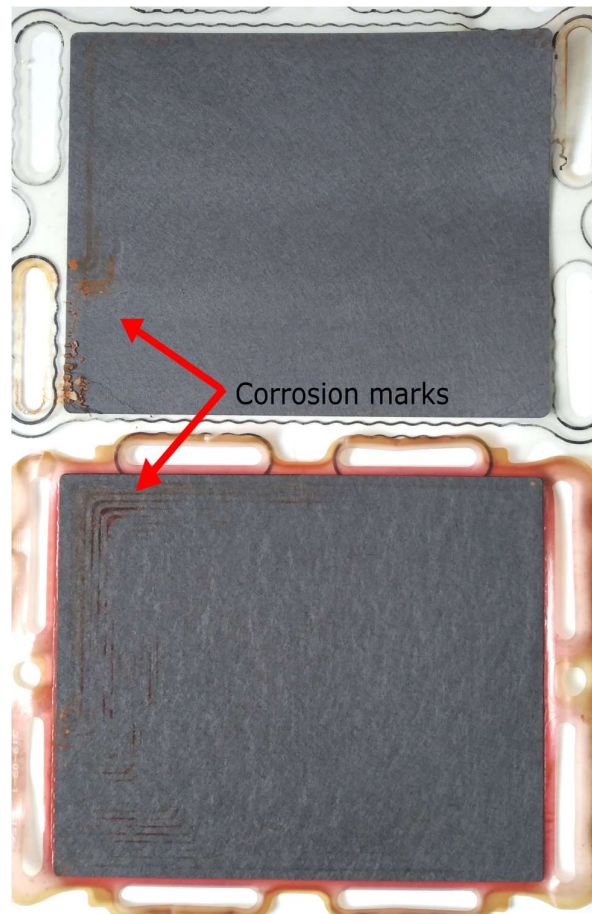


Figure 10. Picture of a cathode membrane electrode assembly contaminated with $5\,000\text{ mg/m}^3$ NaCl (at the top) and another one from a stack operated 50 h in a marine environment (at the bottom), both showing corrosion marks close to the air inlet.

The last part of post-mortem analyses was the measurement of the cathode effluent conductivity. As reported in Table II, the more concentrated was the mist, the higher the conductivity of the effluents collected during the contamination. For a given NaCl rate, the conductivity of the stack effluents was higher than the single cell one. This result is in good agreement with Fe, Ni, and Cr identifications explained above, which very probably contributed largely to this high conductivity measurement. When using a graphite current collector, the conductivity of the effluents collected during the recovery step was not substantially decreased, contrary to the observations made with metal end plates.

Table II. Cathode effluents conductivity measured for several NaCl contamination tests during the baseline recording, the contamination step, and the recovery step.

NaCl amount in the airflow	Cathode current collector or bipolar plates	Baseline ($\mu\text{S}/\text{cm}$)	Contamination ($\mu\text{S}/\text{cm}$)	Recovery ($\mu\text{S}/\text{cm}$)
10 mg/m^3	Gold/copper (single cell)	3.2	60	12
10 mg/m^3 (with intermediate characterizations)	Graphite (single cell)	/	63	54
500 mg/m^3	SS316L (stack)	4.7	5200 (on average)	189

Discussion

Mikkola et al.¹¹ first described PEMFC performance loss when exposed to NaCl. A few recent studies complemented their work, but some observations remain unclear. Therefore, NaCl mist contaminations were carried out on single cells and stacks. Electrochemical tests and post-mortem analyses proved that NaCl not only affects the FC performance but also corrodes the metal plates.

The voltage drop observed when single cells and stacks were exposed to a NaCl mist is consistent with most studies found in the literature.^{11–14} The level of deterioration differed from one work to another, but the impact was notable. Conversely, Baturina et al.²⁶ reported that the NaCl effect was insignificant compared to HCl during 20 h contamination tests. It was assumed that GDL hydrophobicity protected the CCL from saline droplets. This issue can hinder the study of NaCl impact. Fortunately, it did not occur with our setup, nor for authors also using an ultrasonic oscillator.^{13,14} Our work proved that NaCl can cross the GDL, as Cl was detected in CCLs when injecting high levels of contaminant. This was observed for both PEMFC single cells and stacks, with MEAs from different suppliers. The droplets sprayed were potentially smaller when using an ultrasonic vibrator, which enabled the mist to reach CCLs.

PEMFC performance decreased roughly linearly during continuous pollution phases. However, repetitive startups and shutdowns, due to night or weekend breaks, influenced constant current tests. The degradation rate was sometimes minimized, thanks to a partial recovery when restarting the FC. Nevertheless, it resulted several times in performance loss after a weekend break, which was frequently dramatic for graphite CC tests. Lamibrac et al.²⁷ noticed that startups can affect PEMFC lifetime, even when fed with clean air. It seems plausible that the presence of NaCl increases this effect. Indeed, the open circuit voltage was not systematically checked after the single cells shutdown procedure. This could lead to Pt dissolution by the formation of chloroplatinate ions (above 0.74 V),²⁸ thus implying performance degradation during breaks. Yan et al.¹⁴ also stopped their experiments for the night but did not notice such an impact. This supports the idea that the NaCl effect is magnified by the FC startup and shutdown procedures.

Electrochemical characterizations highlighted potential mechanisms involved, especially for stacks. In most cases, polarization curve recording accelerated the degradation. Currents higher than 0.5 A/cm^2 were reached, which could also enhance BPs corrosion. This result is consistent with literature reporting that HCl impact is increased with current density.¹⁷ After the two contamination steps, kinetic and ohmic contributions seemed to limit the overall

PEMFC stack performance on polarization curves.²⁹ Electrodes and membrane damage could be inferred, or an increase in the contact resistance, most probably due to BPs degradation. Conversely, EIS spectra analysis suggest that mass transfer limitation was dominant for the most degraded cell, meaning C5. This was strengthened by an increase in mass transfer resistance. The contact between air and triple points might be reduced because of NaCl presence, but was fortunately mostly recovered after rinsing. A decrease in the hydrophobicity of the cathode GDL can also be assumed, causing flooding issues.^{28,30} The change in permeation current was attributed to a slight rise in H₂ crossover.³¹ It was sufficiently low to assume that the membranes were not drilled, which was consolidated by the excellent performance recoveries mentioned before.

A remarkable outcome of this study was the regeneration phenomena, already reported in Sasank et al. work.¹² Initial performance recovery was observed for the single cell type 1 polluted in a short period, but with highly concentrated NaCl mist. Low voltages were reached after the end of nebulization, which could have resulted in the desorption of Cl⁻ from Pt.²⁸ Concerning long contamination tests with copper CCs, single cells partially recovered their initial performance when humidified with deionized water. Perhaps NaCl remained in the MEA because of stronger interaction due to a longer contamination time, or a degradation process was triggered and continued even under clean water operation. Our observations slightly differ from Li et al. work,¹⁶ reporting partial recovery under pure water after a 4 ppm HCl injection but not after a 20 ppm exposure. The existence of an irreversible mechanism can be inferred, probably linked to Cl⁻ presence. For stacks, the excellent regeneration further outlined a memory effect of contamination. Indeed, the voltage of the most degraded cell decreased as soon as the second NaCl mist exposure began. Characterization steps can also help regeneration, as they were carried out under pure water humidification at the cathode.

Post-mortem analyses provided additional information regarding degradation mechanisms. As described earlier, Cl was systematically found on cathode GDL, so as NaCl for high concentration tests. Furthermore, Cl contaminated the CCL for both single cells and stacks after 10 min and 8 h of 5000 mg/m³ NaCl contamination respectively, followed by a clean mist operation. Thus, the sudden loss of performance can be due to Na⁺ blocking the ionomer sulfonate sites,^{11,21} or/and Cl⁻ directly contaminating, more or less reversibly, the Pt catalyst.^{13,22} Indeed, short contaminations seem to lead to a remarkable recovery of performance thanks to reversible mechanisms. Cl⁻ adsorption/desorption on the catalyst was assumed, and Na⁺ was most probably flushed from the membrane. Longer contaminations can be associated with only partial regeneration, even when low NaCl amounts are introduced. In this case, Pt dissolution, Ostwald ripening, or membrane irreversible degradation might be predominantly involved. Surprisingly, performance recovery was not easily reproduced when using a graphite CC. The striking high values of effluents conductivity during rinsing steps support the idea that NaCl remained in the setup, before being slowly removed by clean water mist.

CC and BP corrosion enhanced by the presence of Cl⁻ should be considered too.³² Indeed, CCs were coated with a thin gold film deposited on a nickel diffusion barrier, which explains the presence of these elements in the MEAs of single cells. Likewise, the systematic Cl presence combined with corroded stainless steel seems to indicate that it was implied in BPs degradation. Corrosion product generation can result in an indirect contamination of the FC. Hongsirikarn et al.³³ reported that Fe³⁺ has a stronger interaction with the membrane sulfonic

sites than H^+ . Moreover, iron cations from BPs corrosion catalyze the Fenton reaction in PEMFC, which causes membrane degradation (F^- loss).^{19,20} In our stack study, corroded particles were largely evacuated in effluents (orange coloration), but some of them could clog the GDL pores and BP channels during the contamination, explaining the mass transport limitation observed. Then, a great part of impurities was probably released with rinsing, explaining the satisfactory regeneration also evidenced by ultimately colorless effluents. However, metal BPs degradation is irreversible, and thus problematic, considering that corrosion also occurred for the stack operated in a marine environment. A means to solve this issue is to use graphite plates. Post-mortem analyses proved that they do not contaminate MEAs, even if graphite is more fragile and heavier.³⁴

Our work confirms that NaCl mist injected in the feeding airflow causes PEMFC degradation, through reversible and irreversible electrochemical processes. Both direct NaCl impact and indirect contamination via plate corrosion are involved, but the results should be interpreted with care. It was difficult to keep stable operating conditions during long contamination tests. Indeed, membrane drying due to temperature control problems led to unavoidable inaccuracies. Furthermore, a few days break sometimes caused restart issues for single cells mounted with a graphite CC, which is problematic for industrial applications. Concerning stacks, there is no clear relationship between the cell position in the stack and the degradation rate. C1 had the highest one for the baseline stack, C4 for the stack exposed to 5000 mg/m^3 NaCl, and C1/C5 for the deeper study at 500 mg/m^3 . This could be explained by fluidic effects, which are particularly visible on the voltage fluctuations of the PEMFC stack contaminated at 5000 mg/m^3 . Channels clogging of one cell seems to trigger a loss of performance that disappears when unclogging, but which then causes another cell to drop in voltage. CV measurements highlighted a slight charge increase after contamination for the weakest cells, which is inconsistent with the literature. Authors usually reported a decrease in ECSA when MEAs were exposed to Cl^- , because of their adsorption on the platinum catalyst.^{13,17,22} Some artifacts caused by H_2 permeation³⁵ or N_2 purge flow rate³⁶ can affect CV measurements, but the characteristics of their voltammograms differed from our own. One very interesting possible explanation is that the electrode geometry might change in the presence of Cl^- . These ions could selectively dissolve Pt particles, and redeposit them in such a way as to create porosity, thus increasing the ECSA.

Future work is planned to address the issues described. Deeper investigations are needed for stacks, including test duplications and longer contaminations. Constant current tests between each electrochemical characterization will help to find out which one can trigger performance recovery. Specific experiments will be carried out to determine the optimal startup, shutdown, and regeneration procedures, first on single cells for a clear understanding. These new tests must include CV measurements to figure out if the catalyst poisoning rate increases with contamination time. Furthermore, CV recordings will be achieved on both sides of single cells to confirm the controversial result observed for PEMFC stacks. The hypothesis of an increase in cathode porosity due to the dissolution of Pt by chlorides should be verified using transmission electron microscopy. XPS should also be considered for studying the electrocatalyst and MPL surfaces and to supplement the information provided by CV and SEM-EDS. Further work will help to know if delaminations are specific to NaCl exposure and if corrosion particles and chlorine remain in the MEA after longer rinsing steps. Moreover, SEM-

EDS observations are needed as well on the membrane to determine if Na^+ or iron ions could be a source of damage. HFR only increased for C1, which is closest to air inlet. It is possible that more NaCl and corrosion products affected the ionomer for this cell. Further interpretation of EIS data is possible through distribution of relaxation times analysis and should be investigated.^{37,38} In the very near future, a 0.1 A/cm^2 constant current test will be accomplished soon to explore the possibility of promoting irreversible degradations under high voltage operation, including Pt dissolution.

Conclusions

In these challenging times, the use of PEMFCs is spreading out for industrial applications. It is therefore necessary to ensure that specific environments will not affect their performance. When fed with marine air, harmful species are introduced into the FC and reach the MEA. In this context, our work focused on the impact of a NaCl mist on PEMFCs, through constant current tests, electrochemical characterizations, and post-mortem analyses. To our knowledge, this study has contributed to the literature in many ways:

- (1) First, it confirmed the significant performance degradation of PEMFC single cells and stacks when exposed to NaCl at various concentrations, for two MEA types. To this end, a dedicated setup was conceived to generate droplets in the micrometer range. Overall, NaCl mist reduces PEMFC lifetime, especially when operated discontinuously.
- (2) An excellent regeneration was obtained for most of the short contaminations, highlighting the existence of a reversible mechanism. Both cathode rinsing with N_2 and clean water operation were successful, including electrochemical characterization steps. For longer contamination tests, with a 10 mg/m^3 NaCl exposure, partial performance recovery was not systematic, suggesting an irreversible process.
- (3) Even if CCL irreversible degradation was not proven, they contained Cl for high NaCl concentrations, which remained after a rinsing step. Na and Cl were both identified on the cathode GDL surface.
- (4) Cl⁻ corroded gas plates for both scales, which led to the formation of metallic impurities reaching the MEA and limiting the mass transportation of gases to the triple point boundaries. Although a good voltage recovery was achieved, BPs were irreversibly damaged, which can lead to an increase in contact resistance.
- (5) A real case study acknowledged the impact of NaCl on PEMFC exposed to a marine environment. 50h of operation did not cause performance loss, but BPs were corroded and Cl was found on the cathode GDL surface. This indicates that the cabin air filter did not block all NaCl particles. Thus, a longer exposure would probably be dramatic, especially if multiple FC stops and restarts are included.

Further study will help to determine if Na^+ is present in the membrane or not, and lower concentrations will be studied to find out an impact threshold. Moreover, CV tests on single cells will help to understand the unclear stacks ECSA observations. Another long-term objective is to find out if longer sea operations result in Cl⁻ reaching the CCL, with the final consequence to reduce the available power. Various filters will be tested, with the aim of adapting them to marine environments.

Acknowledgments

The present work was financially supported by the Pays de la Loire Region. The authors would like to acknowledge the ERIMAT-Capacités team for post-mortem analyses.

References

1. IPCC, *Climate Change 2022: Impacts, Adaptation and Vulnerability*. Contribution of Working Group II to the Sixth Assessment Report of the Intergovernmental Panel on Climate Change [H.-O. Pörtner, D.C. Roberts, M. Tignor, E.S. Poloczanska, K. Mintenbeck, A. Alegría, M. Craig, S. Langsdorf, S. Löschke, V. Möller, A. Okem, B. Rama (eds.)]. Cambridge University Press. Cambridge University Press, Cambridge, UK and New York, NY, USA, 3056 pp. (2022).
2. S. M. S. Privitera, M. Muller, W. Zwaygardt, M. Carmo, R.G. Milazzo, P. Zani, M. Leonardi, F. Maita, A. Canino, M. Foti, F. Bizzarri, C. Gerardi, and S.A. Lombardo, *J. Power Sources*, **473**, 228619 (2020).
3. A. Grimm, W. A. de Jong, and G. J. Kramer, *Int. J. Hydrog. Energy*, **45**, 22545–22555 (2020).
4. D. J. Myers, A. J. Kropf, E. C. Wegener, H. Mistry, N. Kariuki, and Jaehyung Park, *J. Electrochem. Soc.*, **168**, 044510 (2021).
5. M. Chourashiya, R. Sharma, S. Gyergyek, and S. M. Andersen, *Mater. Chem. Phys.*, **276**, 125439 (2022).
6. M. Titirici, S. G. Baird, T. D. Sparks, S. M. Yang, A. Brandt-Talbot, O. Hosseinaei, D. P. Harper, R. M. Parker, S. Vignolini, L. A. Berglund, Y. Li, H.-L. Gao, L.-B. Mao, S.-H. Yu, N. Díez, G. A. Ferrero, M. Sevilla, P. A. Szilágyi, C. J. Stubbs, J. C. Worch, Y. Huang, C. K. Luscombe, K.-Y. Lee, H. Luo, M. J. Platts, D. Tiwari, D. Kovalevskiy, D. J. Fermin, H. Au, H. Alptekin, M. Crespo-Ribadeneyra, V. P. Ting, T.-P. Fellingner, J. Barrio, O. Westhead, C. Roy, I. E. L. Stephens, S. A. Nicolae, S. Ch Sarma, R. P. Oates, C.-G. Wang, Z. Li, X. J. Lo, R. J. Myers, N. Heeren, A. Grégoire, C. Périssé, X. Zhao, Y. Vodovotz, B. Earley, G. Finnveden, A. Björklund, G. D. J. Harper, A. Walton, and P. A. Anderson, *J. Phys. Mater.*, **5**, 032001 (2022).
7. E. Merico, A. Donato, A. Gambaro, D. Cesari, E. Gregoris, E. Barbaro, A. Dinoi, G. Giovanelli, S. Masieri, and D. Contini, *Atmos. Environ.*, **139**, 1–10 (2016).
8. F. Jing, M. Hou, W. Shi, J. Fu, H. Yu, P. Ming, and B. Yi, *J. Power Sources*, **166**, 172–176 (2007).
9. T. Reshetenko, V. Laue, U. Krewer, and K. Artyushkova, *J. Power Sources*, **438**, 226949 (2019).
10. J. Piazzola, K. Sellegri, L. Bourcier, M. Mallet, G. Tedeschi, and T. Missamou, *Atmos. Environ.*, **54**, 545–556 (2012).
11. M. S. Mikkola, T. Rockward, F. A. Uribe, and B. S. Pivovar, *Fuel Cells*, **7**, 153–158 (2007).
12. B. V. Sasank, N. Rajalakshmi, and K. S. Dhathathreyan, *J. Mar. Sci. Technol.*, **21**, 471–478 (2016).
13. S. Uemura, M. Yamazaki, T. Yoshida, T.-C. Jao, and S. Hirai, *ECS Trans.*, **80**, 651–655 (2017).
14. W.-M. Yan, H.-S. Chu, Y.-L. Liu, F. Chen, and J.-H. Jang, *Int. J. Hydrog. Energy*, **36**, 5435–5441 (2011).
15. K. Matsuoka, S. Sakamoto, K. Nakato, A. Hamada, and Y. Itoh, *J. Power Sources*, **179**, 560–565 (2008).
16. H. Li, H. Wang, W. Qian, S. Zhang, S. Wessel, T. T.H. Cheng, J. Shen, and S. Wu, *J. Power Sources*, **196**, 6249–6255 (2011).
17. H. Li, S. Zhang, W. Qian, Y. Yu, X.-Z. Yuan, H. Wang, M. Jiang, S. Wessel, and T. T.H. Cheng, *J. Power Sources*, **218**, 375–382 (2012).
18. A. J. Steinbach, C. V. Hamilton, and M. K. Debe, *ECS Trans.*, **11**, 889–902 (2019).
19. I. Elferjani, G. Serre, B. Ter-Ovanesian, and B. Normand, *Int. J. Hydrog. Energy*, **46**, 32226–32241 (2021).
20. A. Pozio, R. F. Silva, M. De Francesco, and L. Giorgi, *Electrochimica Acta*, **48**, 1543–1549 (2003).

21. X. Cheng, Z. Shi, N. Glass, L. Zhang, J. Zhang, D. Song, Z.-S. Liu, H. Wang, and J. Shen, *J. Power Sources*, **165**, 739–756 (2007).
22. O. A. Baturina, A. Epshteyn, P. Northrup, and K. E. Swider-Lyons, *J. Electrochem. Soc.*, **161**, F365–F372 (2014).
23. S. Kooij, A. Astefanei, G. L. Corthals, and D. Bonn, *Sci. Rep.*, **9**, 6128 (2019).
24. S. Chevalier, J.-C. Olivier, C. Josset, and B. Auvity, *J. Power Sources*, **440**, 227100 (2019).
25. C. Georges, H. Sanchez, N. Semmar, C. Boulmer-Leborgne, C. Perrin, and D. Simon, *Appl. Surf. Sci.*, **186**, 117–123 (2002).
26. O. A. Baturina, P. Northrup, and K. Swider-Lyons, *ECS Meet. Abstr.*, **MA2012-02**, 1299–1299 (2012).
27. A. Lamibrac, G. Maranzana, J. Dillet, O. Lottin, S. Didierjean, J. Durst, L. Dubau, F. Maillard, and M. Chatenet, *Energy Procedia*, **29**, 318–324 (2012).
28. O. A. Baturina, A. Epshteyn, P. A. Northrup, and K. E. Swider-Lyons, *J. Electrochem. Soc.*, **158**, B1198 (2011).
29. M. Jouin, R. Gouriveau, D. Hissel, M.-C. Péra, and N. Zerhouni, *Int. J. Hydrog. Energy*, **38**, 15307–15317 (2013).
30. H. Nakajima, T. Kitahara, and K. Dan, *ECS Trans.*, **92**, 341–349 (2019).
31. S. Wasterlain, D. Candusso, F. Harel, D. Hissel, and X. François, *J. Power Sources*, **196**, 5325–5333 (2011).
32. J. André, L. Antoni, and J.-P. Petit, *Int. J. Hydrog. Energy*, **35**, 3684–3697 (2010).
33. K. Hongsirikarn, J. G. Goodwin, S. Greenway, and S. Creager, *J. Power Sources*, **195**, 7213–7220 (2010).
34. P. Bujlo, C. Cornelius, O. Barron, N. Dyantyi, V. Linkov, and S. Pasupathi, *Int. J. Hydrog. Energy*, **46**, 29478–29487 (2021).
35. M. Edmundson and F. C. Busby, *ECS Trans.*, **41**, 661–671 (2011).
36. R. N. Carter, S. S. Kocha, F. Wagner, M. Fay, and H. A. Gasteiger, *ECS Trans.*, **11**, 403–410 (2007).
37. Q. Meyer, S. Liu, Y. Li, and C. Zhao, *J. Power Sources*, **533**, 231058 (2022).
38. S. Dierickx, A. Weber, and E. Ivers-Tiffée, *Electrochimica Acta*, **355**, 136764 (2020).